Robust MPC for Steering Assist Control with Uncertain Driver Model

Rohit Ravikumar
rraviku@clemson.edu

Saumil Vikas Pradhan
saumilv@clemson.edu

Vasudev Purohit
vpurohi@clemson.edu

***Abstract*— Recent advancements in advanced driver assistance systems have helped mitigate human error, apart from laying the down the path for full-autonomous vehicle acceptance. Steering assist systems are capable of interventions that overwrite or correct the driver's input. This project outlines such an ADAS system that can be used for lane-keeping and obstacle avoidance of semi-autonomous ground vehicle. A closed-loop system considering the vehicle and the uncertain driver is used. A tube-based predictive control framework is used to ascertain that the system safety constraints are met at all times, while organically complementing the driver's inputs.**

***Index Terms*—Advanced driver assistance systems, robust model predictive controller, optimal control, steering assist, active safety, tube-based model predictive controller**

NOMENCLATURE

β	Vehicle Side Slip Angle
δ	Driver Steering Input
Δy	Vehicle lateral deviation
ψ	Vehicle orientation
C_1	Front tire cornering stiffness
C_2	Rear tire cornering stiffness
C_{Mz1}	Front tire aligning stiffness
C_{Mz2}	Rear tire aligning stiffness
x_{fpi}	Vehicle footprint X for i^{th} corner, t=0
x'_{fpi}	Vehicle footprint X for i^{th} corner at any t
y_{fpi}	Vehicle footprint Y for i^{th} corner, t=0
y'_{fpi}	Vehicle footprint Y for i^{th} corner at any t
a	CG to front axle distance
ADAS	Advanced Driver Assistance System
b	CG to rear axle distance
HMM	Hidden Markov Model
LC/CA	Collision Avoidance
m	Vehicle mass
MPC	Model Predictive Control
MPT	Multi-Parametric Toolbox
mRPI	Maximal Robust Positive Invariant set
r	Yaw rate
TLC	Time to Line Crossing
V	Vehicle Velocity
X	Vehicle CG X in global frame
Y	Vehicle CG Y in global frame

I. INTRODUCTION

There has been a great deal of importance laid on the safety of the passengers, and rightly so. Even though it is difficult to pinpoint the reason for the occurrences of these accidents, it is agreed that driver distraction contributes majorly to all the crashes. Rise in ADAS has led to safer vehicles, and have been helping auto-makers tremendously in the race for full-autonomous acceptance amongst its customers.

Human factors research with body sensors and driver behavior prediction [1] faces integration challenges with ADAS controllers. A commercial lane departure detection method [2], [3] estimates the lane departure time and initiates an intervention but has limitations, including a hard-coded TLC threshold and reliance on unmeasurable lateral acceleration.

Some research communities addressing this issue employ complex models [4], [5], [13] to predict uncertain driver behavior and enhance system reliability. But these approaches rely heavily on driving data.

To tackle the challenge of complex driver models, [8] employs a simpler approach by treating driver inputs as disturbances and combining them with vehicle models similar to those in [4] and [5]. This fusion aids in identifying precursor safe states, that the vehicle should be at, aimed at reaching a predetermined terminal target set. In contrast, [9] employs a forward reachable set calculation to determine the need for steering assistance in LC/CA maneuvers. This work builds upon [8] by introducing additive uncertainty into driver inputs, acknowledging their non-deterministic nature. A tube-based predictive controller, while acting on tightened constraints, operates continuously but provides an 'aiding' steering input only when it predicts that the driver's inputs, accounting for uncertainty, may fall short in executing the desired LC/CA maneuver. Various methods of constraint tightening have been employed and discussed in this report. An ancillary controller is employed to keep the actual trajectory of the states close to the trajectory of the nominal system.

II provides a high-level overview of our project's approach. In III, we present the plant models for our formulations, while IV delves into the tube-based MPC and tightened safety constraints formulation, guiding our intervention strategies. VI discusses the results obtained through this implementation. VII outlines the shortcomings of our project and the steps that can be taken to solve these problems, as an extension to the project.

II. METHODOLOGY

The issue addressed in I has been systematically tackled through the deployment of a tube-based model predictive control (MPC) framework. The introduction of robustness is

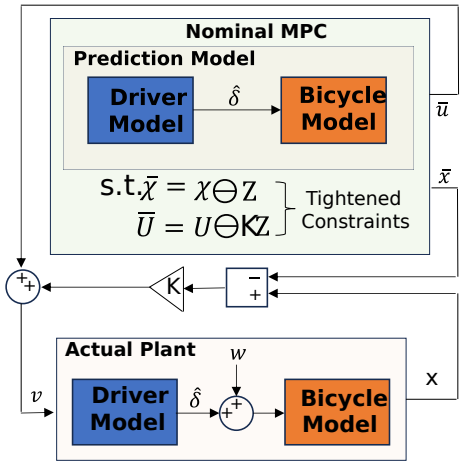

Fig. 1: Block diagram representing the tube-based MPC used as a steering assist controller. The nominal MPC acts on the nominal plant and tightened constraints. The ancillary controller keeps the actual trajectory close to the nominal trajectory.

imperative owing to the inherent uncertainty characterizing the driver model. The utilized plant model corresponds to a closed-loop configuration comprising both driver and vehicle dynamics. Specifically, the vehicle is represented by a bicycle model, while the driver functions as a yaw-controller featuring bounded additive uncertainties. Detailed formulations of the governing equations for the plant model are explicated in the dedicated section labeled III.

The implemented control strategy employs a tube-based MPC approach, chosen for its ability to enhance robustness and guarantee constraint satisfaction. The tube-based MPC utilizes a cascaded framework, consisting of a nominal MPC responsible for generating optimal control input ($\bar{u}$) based on a nominal plant model, with tightened safety constraints. Additionally, an ancillary controller (1) is incorporated to ensure that the actual plant trajectory (x) closely follows the nominal plant trajectory ($\bar{x}$). The gain feedback gain K in was chosen as the LQR controller gain for the system, but can also be found using other techniques e.g., pole-placement. The control action acting on the plant is then the sum of the two, defined in (1).

$$v(t) = \bar{u}(t) + K_{LQR}(x(t) - \bar{x}(t)) \tag{1}$$

The nominal MPC is continually active, employing the nominal system as its predictive model, as previously discussed, albeit with tightened constraints on both states and control inputs. The definition of these tightened constraints represented by polytopes is facilitated through the computation of the outer-approximation of robust positive invariant set, often referred to as a disturbance invariance set ($\mathcal{Z}$). The foundation for the robust actions as elucidated in [8] is rooted in two key propositions:

- The existence of a control law (1) that, when applied, ensures the system, even in the presence of disturbances, remains confined within the disturbance invariant set centered around the nominal states i.e.,

$$x(0) \in \{\bar{x}_0\} \oplus \mathcal{Z} \Rightarrow x(t) \in \{\bar{x}_t\} \oplus \mathcal{Z} \;\; \forall w(t) \in \mathcal{W}, \;\; \forall t \geq 0 \tag{2}$$

- The size of this tube is established through an estimation of the disturbance invariant set ($\mathcal{Z}$), often referred to as the mRPI set. The determination of the set's size is described in V. Subsequently, the tightened constraints on states ($\bar{\mathcal{X}}$) and control inputs ($\bar{\mathcal{U}}$), used by the nominal MPC, can be found out by (3) & (4).

$$\mathcal{X} = \bar{\mathcal{X}} \oplus \mathcal{Z} \Rightarrow \bar{\mathcal{X}} = \mathcal{X} \ominus \mathcal{Z} \tag{3}$$

$$\mathcal{U} = \bar{\mathcal{U}} \oplus \mathcal{K}\mathcal{Z} \Rightarrow \bar{\mathcal{U}} = \mathcal{U} \ominus \mathcal{K}\mathcal{Z} \tag{4}$$

$\mathcal{W}$ represents the set containing the disturbances. These disturbances are assumed to be bounded in the entire formulation.

As an alternate method, the constraint tightening can also be carried out by scaling down the constraints using an appropriate scaling factor, to both, the state and control input constraints. The details of this method have also been described in V.

III. Plant Model

A. Vehicle Model & Driver Closed Loop Model

The underlying linear bicycle model employed in this investigation describing the vehicle dynamics has been adopted from [11]. The linearization of the non-linear vehicle model was carried out by assuming a linear tire model. This results in an affine relationship between the tire's cornering stiffness and the lateral force generated by it. Furthermore, small angle approximation was needed to linearize the model. Since the aim of this ADAS system is to complement the driver for LC/CA maneuvers, the states of the driver as yaw controller are also included as part of the plant model. Thus, the combined states of the plant model are β, r, δ, ψ and Δy. Y_β, Y_r, Y_δ, N_β, N_r, and N_δ are the derivatives of stability. The ancillary control action v, obtained via the robust control law (1), is a steering angle and hence affects only the first two states.

$$\begin{aligned}
Y_\beta &= -(C_1 + C_2) \\
Y_r &= -\frac{1}{V}(aC_1 - bC_2) \\
Y_\delta &= C_1 \\
N_\beta &= -aC_1 + bC_2 + C_{Mz1} + C_{Mz2} \\
N_r &= \frac{1}{V}(-a^2C_1 - b^2C_2 + aC_{Mz1} - bC_{Mz2}) \\
N_\delta &= aC_1 - C_{Mz1} \\
\dot{\beta} &= \frac{Y_\beta}{mV}\beta + \frac{Y_r - mV}{mV}r + \frac{Y_d}{mV}(\delta + v) \\
\dot{r} &= \frac{N_\beta}{J_z}\beta + \frac{N_r}{J_z}r + \frac{N_d}{J_z}(\delta + v) \\
\dot{\delta} &= -\frac{1}{\tau}\delta - \frac{K_d}{\tau}\psi - \frac{K_d}{L_a\tau}\Delta y + \frac{K_d}{\tau}\psi_{ref} \\
\dot{\psi} &= r \\
\Delta\dot{y} &= V\beta
\end{aligned} \tag{5}$$

The vehicle parameters used in equation 5 are described in Table I of appendix A. The driver parameters comprise of the driver gain (K_d), reaction delay (τ) and the lookahead distance (L_a). The values of these have also been described in Table I of appendix A.

The ψ_{ref} refers to the reference vehicle orientation for the maneuvers chosen in this report. A lane change maneuver - corresponding to avoiding one obstacle has been generated offline. For the online determination of ψ_{ref}, a lookup table was employed for the values generated offline.

As mentioned in Section II, the driver input under consideration in this report is characterized by inherent uncertainty. Specifically, the driver's actual steering input is derived from a sum of the nominal driver model and an additive disturbance that is bounded by $\mathcal{W}$.

$$\delta_d \in \left\{ \hat{\delta}_d \oplus \mathcal{W}_\delta \right\} \subseteq \mathbb{R} \tag{6}$$

The values for bounds on additive driver disturbances have also been mentioned in table I of appendix A.

Since the position of obstacle and lane-lines, and hence the safety constraints are defined in the global frame of reference, a track of the vehicles' footprint in the global frame of reference is also maintained. These are obtained by defining a transformation matrix (7). (i=0 to 4 for all 4 corners of the vehicle).

$$\begin{bmatrix} x'_{fpi} \\ y'_{fpi} \\ 1 \end{bmatrix} = \begin{bmatrix} cos(\psi) & -sin(\psi) & X \\ sin(\psi) & cos(\psi) & Y \\ 0 & 0 & 1 \end{bmatrix} \begin{bmatrix} x_{fpi} \\ y_{fpi} \\ 1 \end{bmatrix} \tag{7}$$

IV. Controller Formulation

A. Nominal MPC

The nominal MPC is designed to be always active, but producing an output solely in response to the scenario when the employed vehicle & driver closed loop model, described in III-A, potentially collides with an obstacle. This design offers the distinct advantage of ensuring continuous controller activity and ascertains no safety-constraint violation. The predictive model utilized for the nominal MPC aligns with the plant model explicated in Section III. The control action exerted by the MPC corresponds to a steering input that serves as assistance, influencing solely the initial two states of the plant, namely, vehicle side slip angle and the vehicle's yaw rate. Consequently, the prediction model can be encapsulated by (8). Only the equations for β and r change, while the rest remain the same.

$$\begin{aligned} \dot{\beta} &= \frac{Y_\beta}{mV}\beta + \frac{Y_r - mV}{mV}r + \frac{Y_d}{mV}(\delta + \bar{u}) \\ \dot{r} &= \frac{N_\beta}{J_z}\beta + \frac{N_r}{J_z}r + \frac{N_d}{J_z}(\delta + \bar{u}) \end{aligned} \tag{8}$$

The cost function of the nominal MPC, as detailed later in this section, incorporates a metric associated with the proximity of the vehicle's footprint to the lanes and obstacle specified within the driving scenario. This assessment of distances is iteratively performed at each step of the predictive horizon. Specifically, the minimum distance between a designated corner of the vehicle (considered as a point) and a line segment representing the side of an obstacle or lane is calculated. The minimum distance between a vehicle's corner and a lane or obstacle is contingent upon the position of the point relative to the line segment. If the point resides within the segment's endpoints, the minimum distance is equivalent to the perpendicular distance between the point and the line segment. Conversely, when the point is located outside the segment, the minimum distance is determined by the distance between the point and the closest endpoint of the segment. In a previous iteration of this distance calculation, the obstacle and lanes were defined as polyhedra, and the minimum distance was determined using the 'distance' property inherent in the polyhedra object within the MPT toolbox. Due to the inability to vectorize this approach, this computation took a longer time and hence former approach was used, also described in figure 2. The distance-dependent costs in the aforementioned calculation are determined through the application of decaying exponential functions (9). The decay rate parameter is fine-tuned to regulate the aggressiveness of cost growth, optimizing the performance of the nominal MPC. The fact that such a cost function is also easily differentiable, it helps the optimization solver to easily calculate the cost function gradients, thereby facilitating efficient optimization processes.

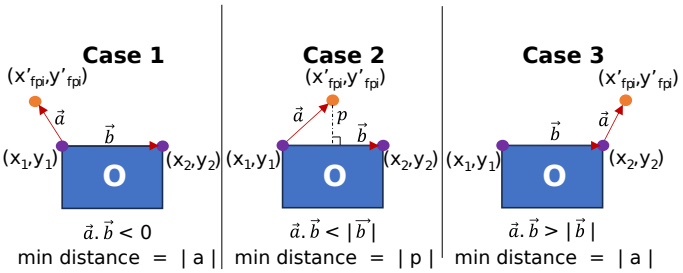

Fig. 2: (x'_{fpi}, y'_{fpi}) represent a given corner of the vehicle footprint at any given time. (x_1, y_1) & (x_2, y_2) are the corners of a lane or the side of an obstacle. The minimum distance between a vehicle's corner and a lane or obstacle is contingent upon the position of the point relative to the line segment. The least distance out of the 4 corners is chosen as the d_{obs} or d_{lane}

$$\begin{aligned} cost_{obstacle} &= e^{-0.5 d_{obs}} \\ cost_{lane} &= e^{-5 d_{lane}} \end{aligned} \tag{9}$$

The cost function (10) is also formulated in a way such that minimal control action is produced, i.e., minimal interventional action is taken. This is done to prevent chances of conflicting inputs given by the driver and the controller. No terms on state-tracking are added to the cost function because the aim of the MPC is to prevent constraint violations only. The safety constraints of obstacle avoidance and lane-keeping and are set up as soft-constraints, and not as hard constraints. These were not implemented as hard constraints solely because we kept running into solver issues. High penalties are assigned

to these costs accordingly. The MPC parameters are mentioned in table II of Appendix B.

$$\begin{aligned}
&\min \bar{u} \sum_{k=0}^{N-1} \|\bar{u}_{t+k,t}\|^2_{R_u} + \|\triangle\bar{u}_{t+k,t}\|^2_{R_{\Delta u}} + \\
&\|cost_{obstacle}\|_{Q_{obstacle}} + \|cost_{lane}\|_{Q_{lane}} \\
&s.t.\ \bar{x}_{t+k+1,t} = f_{dm}(\bar{x}_{t+k.t}, \bar{u}_{t+k.t}), \\
&\bar{u}_{t+k,t} = \triangle\bar{u}_{t+k,t} + \bar{u}_{t+k-1,t}, \\
&\bar{u}_{t+k,t} \in \bar{\mathcal{U}},\ \ \triangle\bar{u}_{t+k,t} \in \triangle\bar{\mathcal{U}}, \\
&\bar{u}_{t-1,t} = \bar{u}(t-1),\ \ \bar{x}_{t,t} = \bar{x}(t)
\end{aligned} \tag{10}$$

The tightened constraints on control inputs and the tightened position for obstacle and lane lines, used for solving the optimization problem defined above, are found out using the process described in V.

B. Ancillary Controller

The ancillary controller, as delineated in Section II, fulfills the critical role of maintaining proximity between the real trajectory of the system and its nominal trajectory. This task is accomplished through the application of the robust control law specified by Equation 1. The feedback gain, denoted by K, serves as a pivotal parameter determining the degree to which the actual trajectory adheres to the nominal trajectory. Consequently, the value of K directly influences the system's ability to remain close to the nominal states, and hence the spread of the actual trajectories.

The feedback gain, denoted as K, has been selected as the Linear Quadratic Regulator (LQR) controller gain within the closed-loop system encompassing the vehicle-driver-nominal MPC system. The performance of the controller is predominantly influenced by the Q and R gains associated with the LQR formulation. As explained in Section VI, the R

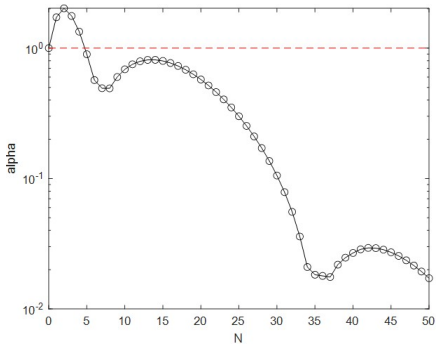

Fig. 3: α v/s N curve obtained by iterating through different values of N and using equation 11. Any value of N can be chosen s.t., the corresponding value of α remains persistently less than 1. N and α are then used to estimate the outer approximation of the mRPI set (S(k,α))

matrix plays a pivotal role in determining the magnitude of the auxiliary controller action. Given the constraint that the intervening action must not be too high in contrast to the driver's inputs, owing to the driver's comfort or sense of control on the vehicle, the R matrix has been judiciously configured to align with these requirements.

V. Constraint Tightening

In the context of tube-based MPC, the fundamental concept revolves around ensuring that the nominal system adheres to tightened constraints, thereby emphasizing the significance of constraint tightening. This involves estimating the mRPI set or, at the very least, an outer approximation ($S_K(\alpha, N)$) of it. The outer approximation of the mRPI set is determined through the utilization of equation (11). A_K is the A matrix for the closed loop system via the choice of a given K, and represents the growth of uncertainties. $\oplus$ represents the Minkowski sum. This approximation depends upon the values of alpha and N. Given that the uncertainties introduced are additive and confined within a boxed region, equation (12) can be used to determine the values of alpha through an iterative exploration of various N. Any value of N for which α persistently stays less than 1 can be chosen. Figure 3 represents the values of α obtained for a sweep of N.

$$S_K(N) = \sum_{i=0}^{N-1} A_K^i \mathcal{W} = A_K^0\mathcal{W} \oplus A_K^1\mathcal{W} \oplus .....A_K^{N-1}\mathcal{W}$$
$$S_K(\alpha, N) = (1-\alpha)^{-1} S_K(N) \tag{11}$$

$$\alpha = max\left(\frac{max_{w\in\mathcal{W}}\|A_K^N w\|_\infty}{max_{w\in\mathcal{W}}\|w\|_\infty}, \frac{max_{w\in\mathcal{W}}\|KA_K^N w\|_\infty}{max_{Kw\in\mathcal{W}}\|w\|_\infty}\right) \tag{12}$$

Despite the calculation of α and N needed for the mRPI set estimation, the 'N' Minkowski sums were causing to be computationally expensive in the constraint tightening process, and hence a more straightforward process was followed - scaling down the state and control constraints by a given factor (13).

$$\begin{aligned}
\bar{\mathcal{X}} &= \theta\mathcal{X} \\
\bar{\mathcal{U}} &= \gamma\mathcal{U}
\end{aligned} \tag{13}$$

VI. Results

First the ancillary controller gain K is tuned. An LQR controller gain is employed for the vehicle-driver-MPC closed-loop system, as detailed II. The parameterization involved selecting different values for Q and R to achieve the K_{LQR} gains, influencing tracking performance. In conducting simulations with a chosen Q and R, specifically with a small R value (R=1), it was observed across 100 disturbance sequences that the actual vehicle trajectories consistently adhered to constraints (Fig 4). However, an unintended consequence emerged—the ancillary controller exhibited excessively high action, as seen in Fig. 5. This can result in making it very difficult to drive.

In the subsequent analysis, same disturbance sequences were simulated with a gain K_{LQR} corresponding to an R value of 100, indicating an increased penalty on controller action. The outcomes, illustrated in Fig 4, show a wider dispersion in actual trajectories, leading to 8 violations among the 100 simulated trajectories. These violations can be attributed to

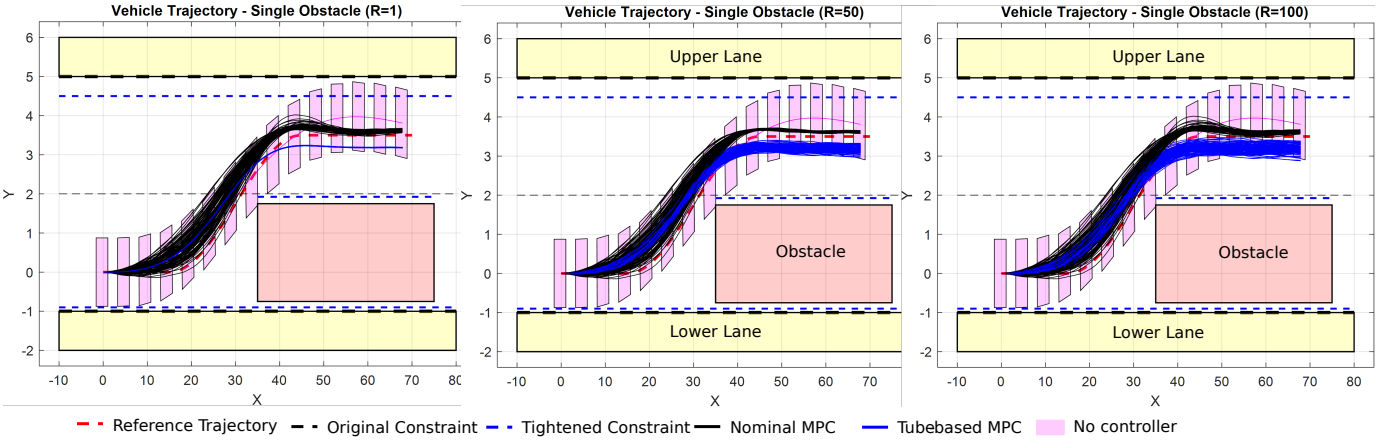

Fig. 4: Ancillary controller gain K tuning. Increasing the R value widens the actual trajectories, thereby increasing the chance of constraint violation. The three figures correspond to simulating the system with the same 100 disturbance sequences.

how well the actual states track the nominal states, and also the fact that the safety constraints have been implemented as soft constraints. However, the elevated R value effectively reduced the ancillary controller actions, as demonstrated in Fig 5. This underscores the trade-off between trajectory robustness and controller action, emphasizing the significance of tuning the penalty parameters for optimal system performance.

In response to eight identified violations, we iteratively adjusted the K_{LQR} gain to mitigate constraint breaches, ultimately selecting an R value of 50 as a balanced compromise between constraint violation and intervention magnitude. This refined K_{LQR} value significantly reduced violations, resulting in only one instance among 100 disturbance sequences. Consequently, this optimized K_{LQR} gain was adopted for the ancillary controller. The performance evaluation also demonstrated satisfactory results in terms of tracking actual states in alignment with nominal ones.

With the tightened constraints and the chosen ancillary controller gain K_{LQR}, the result for a given disturbance sequence, the resulting trajectory looks as shown in Fig. 6. The scenario is set up in such a way that the vehicle and driver-in-loop model with no ADAS controller collides with an obstacle. The system with the tube-based MPC in loop avoids the obstacle with minimal intervention. (Fig. 7).

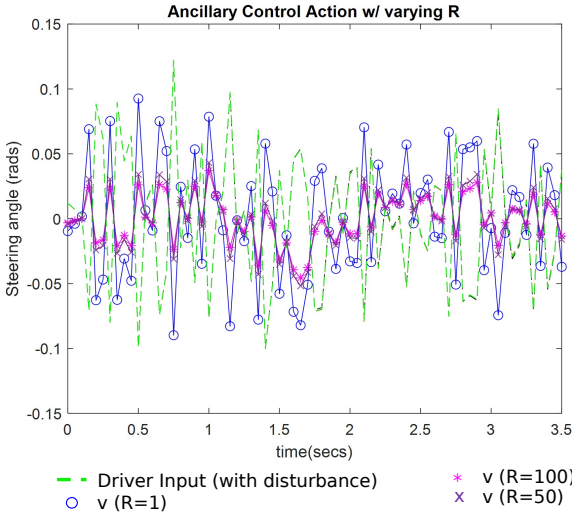

Fig. 5: Ancillary controller action with changing values of R for a single disturbance sequence. Increasing the R for ancillary controller gain K_{LQR} reduces the magnitude of the intervening action. Results shown for one of 100 disturbance sequences simulated.

VII. Conclusion & Future Scope

The uncertainty considered in this project was only additive in nature. However, the uncertainty in driver model can also be parameteric, with the parameters describing the driver, namely K_d, L_a and τ being uncertain. A tube-based MPC considering these uncertainties can also be designed.

The constraint tightening process was carried out iteratively, rather than via a proper analysis. An attempt was made to find out the mRPI set, but the result yielded inconclusive. Hence, the team would like to take this up as part of the future scope of this project.

The obstacle being considered throughout the scope of this project were considered stationary. For highway applications, the obstacles are seldom stationary. Hence an extension to accommodate dynamic obstacles can also be considered and studied further.

Conclusively, the team was able to demonstrate the use of a tube-based MPC for a steering-assist application. The vehicle and driver model was chosen as the plant, with an additive disturbance to the steering angle provided by the driver. For the tube-based MPC, a nominal MPC was designed to intervene only when the vehicle+driver model predicted a constraint violation. An ancillary controller was designed using a robust control law, with the feedback gain chosen as the K_{LQR} gain of the vehicle-driver and MPC in loop model. Different values of K were iterated for constraint satisfaction and minimal interventional action. The resultant controller was simulated

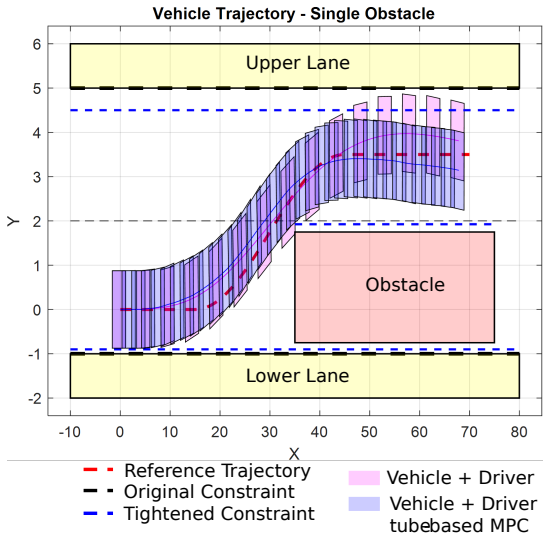

Fig. 6: Trajectories comparing a vehicle with no ADAS controller v/s the one equipped with the controller described in this report.

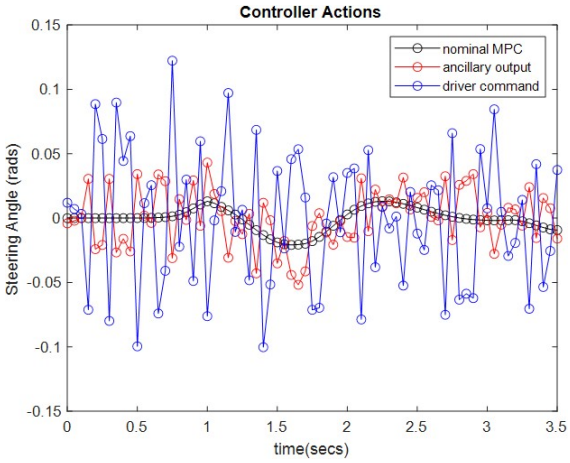

Fig. 7: Comparison of the driver commands (with added disturbance), nominal MPC action, and ancillary controller action. It can be noted that the nominal MPC kicks in only when the vehicle+driver model predicts a constraint violation.

for over 100 disturbance sequences.

REFERENCES

[1] Sathyanarayana, A., Nageswaren, S., Ghasemzadeh, H., Jafari, R., and Hansen, J. H. (2008, September). Body sensor networks for driver distraction identification. In 2008 IEEE international conference on vehicular electronics and safety (pp. 120-125). IEEE

[2] J.Gayko, Handbook of intelligent vehicles. Springer,2012,ch.Lane departure and lane keeping,pp.689–708.

[3] Mammar, S., Glaser, S., and Netto, M. (2006). Time to line crossing for lane departure avoidance: A theoretical study and an experimental setting. IEEE Transactions on intelligent transportation systems, 7(2), 226-241.

[4] Lefevre, S., Gao, Y., Vasquez, D., Tseng, H. E., Bajcsy, R., and Borrelli, F. (2014). Lane keeping assistance with learning-based driver model and model predictive control. In 12th International Symposium on Advanced Vehicle Control.

[5] Vasudevan, R., Shia, V., Gao, Y., Cervera-Navarro, R., Bajcsy, R., and Borrelli, F. (2012, June). Safe semi-autonomous control with enhanced driver modeling. In 2012 American Control Conference (ACC) (pp. 2896-2903). IEEE.

[6] Yan, F., Eilers, M., Lüdtke, A., and Baumann, M. (2016, June). Developing a model of driver's uncertainty in lane change situations for trustworthy lane change decision aid systems. In 2016 IEEE Intelligent Vehicles Symposium (IV) (pp. 406-411). IEEE.

[7] Mayne, D. Q., Seron, M. M., and Raković, S. V. (2005). Robust model predictive control of constrained linear systems with bounded disturbances. Automatica, 41(2), 219-224.

[8] Falcone, P., Ali, M., and Sjoberg, J. (2011). Predictive threat assessment via reachability analysis and set invariance theory. IEEE Transactions on Intelligent Transportation Systems, 12(4), 1352-1361.

[9] Gray, A., Gao, Y., Hedrick, J. K., and Borrelli, F. (2013, June). Robust predictive control for semi-autonomous vehicles with an uncertain driver model. In 2013 IEEE intelligent vehicles symposium (IV) (pp. 208-213). IEEE.

[10] Schnelle, S., Wang, J., Jagacinski, R., and Su, H. J. (2018). A feed-forward and feedback integrated lateral and longitudinal driver model for personalized advanced driver assistance systems. Mechatronics, 50, 177-188.

[11] Althoff, M., and Dolan, J. M. (2011, October). Set-based computation of vehicle behaviors for the online verification of autonomous vehicles. In 2011 14th International IEEE Conference on Intelligent Transportation Systems (ITSC) (pp. 1162-1167). IEEE.

[12] Althoff, M., Stursberg, O., and Buss, M. (2008, December). Reachability analysis of nonlinear systems with uncertain parameters using conservative linearization. In 2008 47th IEEE Conference on Decision and Control (pp. 4042-4048). IEEE.

[13] Herceg M., Kvasnica, M, Jones,C.N and M. Morari, M (2013, July). Multi-Parametric Toolbox 3.0. In Proc. of the European Control Conference (pp. 502-510).

APPENDIX A
PLANT MODEL PARAMETERS

TABLE I: Vehicle Driver Parameters

Parameter	Unit	Value
Vehicle mass(m)	kg	1550
Rotational moment of inertia(J_z)	kg-m^2	2000
CG to front axle (a)	m	1.064
CG to rear axle (b)	m	1.596
Vehicle track-width	m	1.75
Front tire cornering stiffness (C_1)	kN/rad	183.34
Rear tire cornering stiffness (C_2)	kN/rad	57.29
Front tire aligning stiffness (C_Mz1)	kN-m/rad	14.89
Rear tire aligning stiffness (C_Mz2)	kN-m/rad	6.87
Vehicle velocity (V)	m/s	19.44
Driver gain (K_d)	-	0.09
Driver time-delay (τ)	-	0.15
Lookahead distance (L_a)	m	22
Additive disturbance ($\mathcal{W}$)	rads	[-0.1 0.1]

APPENDIX B
CONTROLLER PARAMETERS

TABLE II: Controller Parameters

Parameter	Unit	Value
Time step	s	0.05
Time horizon	s	0.75
Horizon length	-	15
$R_{\Delta u}$	-	50
R_u	-	50
$Q_{obstacle}$	-	1
Q_{lane}	-	1
θ	-	0.2
γ	-	0.1